Numerical simulations for Virgo O3 NCal using FROMAGE

D. Estevez, B. Mours, T. Pradier
IPHC

VIR-0759A-20

Contents

Introduction

FROMAGE[1] is a new simulation tool developed for gravitational effects induced by rotating masses using a Finite Element Analysis (FEA) and written in C/C++. It can be found in the Git repository: https://git.ligo.org/virgo/virgoapp/FROMAGE
This note reports new simulations for the Virgo NCalO3[2] using the version v1r0 of FROMAGE. The numerical results obtained are compared to new analytical results derived in this note. We improved the previous analytical model to include a correction for an extended mirror along the longitudinal and radial directions when the NCal is in the interferometer plane and makes an angle ϕ with the ITF beam axis.

1 Analytical model for the NCal-induced mirror motion

1.1 Amplitude of the mirror motion at the order 4 for an extended mirror and an extended rotor

The amplitude of the mirror motion has been computed for an extended rotor and an extended mirror in the radial dimension (see VIR-0268A-20). The correction factor for the extension of the mirror was not accurate and we report here a correction to the previous computation adding also a correction term for the longitudinal dimension of the mirror. We recall the sketch of the considered situation in Figure 1.

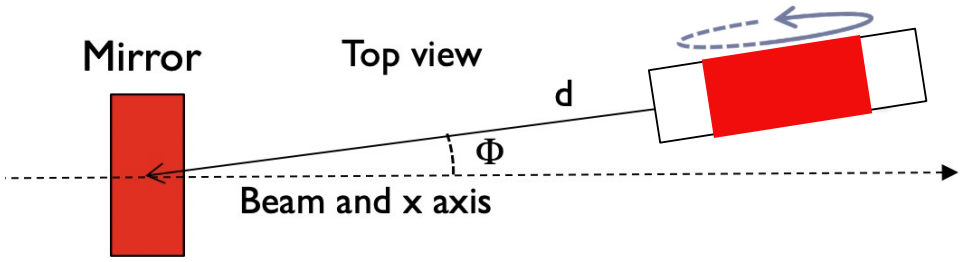

Figure 1: Top view sketch of the NCal rotor made of two sectors making an angle ϕ with the extended mirror.

We consider the sectors of the rotor located at:

$$(d\cos(\phi) \pm r\cos(\theta)\cos(\phi); d\sin(\phi) \pm r\cos(\theta)\sin(\phi); \pm r\sin(\theta))$$

[1] Finite element analysis of ROtating MAsses for Gravitational Effects
[2] Previously called NCal200

and a point in the extended mirror located at $(x; r'\cos(\beta); r'\sin(\beta))$. The longitudinal force induced by one mass of the rotor expanded at the 4-th order in $\epsilon = \frac{r}{d}$, $\epsilon' = \frac{r'}{d}$ and $\epsilon'' = \frac{x}{d}$ is :

$$\begin{aligned} F_{1x} &= \frac{GmM}{d^4}(\cos(\phi) + \epsilon\cos(\theta)\cos(\phi) - \epsilon'')\Big[1+X\Big]^{-3/2} \\ &\approx \frac{GmM}{d^4}(\cos(\phi) + \epsilon\cos(\theta)\cos(\phi) - \epsilon'')\Big[1 - \frac{3}{2}X + \frac{15}{8}X^2 - \frac{35}{16}X^3 + \frac{315}{128}X^4\Big] \end{aligned} \tag{1}$$

where $X = \epsilon^2 + \epsilon'^2 + \epsilon''^2 + 2\epsilon\cos(\theta) - 2\epsilon'\cos(\phi)(1+\epsilon\cos(\theta)) - 2\epsilon''\sin(\phi)\cos(\beta)(1+\epsilon\cos(\theta)) - 2\epsilon\epsilon''\sin(\beta)\sin(\theta))$

After some tedious computations keeping only the terms up to the fourth order and using a similar approach to compute the longitudinal force F_{2x} for the second mass of the rotor we get the amplitude of the total longitudinal force F_x at $2f_{rot}$. However for clarity reasons due to the numerous number of terms, we already discard terms containing odd powers of either $\cos(\beta)$, $\sin(\beta)$ or ϵ'' since the integration that will be performed further cancels these terms:

$$\begin{aligned} F_x \approx \frac{9GmMr^2}{2d^4}\Big[&\cos(\phi) + \frac{25}{36}\cos(\phi)\epsilon^2 \\ &+ \Big(\Big(\frac{405}{18}\sin^2(\phi) + \frac{15}{9}\Big)\cos(\phi)\cos^2(\beta) - \frac{105}{18}\cos(\phi)\Big)\epsilon'^2 \\ &+ \Big(\frac{51}{9}\cos^2(\phi) - \frac{15}{9}\Big)\epsilon'' + \Big(\frac{405}{18}\cos^3(\phi) - \frac{225}{18}\cos(\phi)\Big)\epsilon''^2\Big]\cos(2\theta) \end{aligned} \tag{2}$$

Let's write the mass of the rotor as:

$$m = \rho_{al}\int\int\int r\ dr\ \cos(2\psi)d\psi\ db$$

and the mass of the mirror as:

$$M = \rho_{mir}\int\int\int r'\ dr'\ d\beta\ dx$$

In order to get the total force for an extended rotor and an extended mirror, Eq. 2 must be integrated over r from r_{min} to r_{max}, r' from 0 to r_{mir}, x from $\frac{-x_{mir}}{2}$ to $\frac{-x_{mir}}{2}$ and β from 0 to 2π. Then, for frequency above the resonance of the mirror suspension ($f \gg 0.6$ Hz) the amplitude of the mirror motion is given by:

$$a(f_{2rot}) = \frac{|F_x|}{M(2\pi f_{2rot})^2} \tag{3}$$

The resulting amplitude is thus:

$$\begin{aligned} a(f_{2rot}) = \frac{9G\rho_{al}\ b\ \sin(\alpha)(r_{max}^4 - r_{min}^4)}{32\pi^2 f_{2rot}^2 d^4}\cos(\phi)\Big[1 + \frac{25}{54d^2}\frac{(r_{max}^6 - r_{min}^6)}{(r_{max}^4 - r_{min}^4)} \\ + \Big(\frac{405}{72}\sin^2(\phi) - \frac{5}{2}\Big)\Big(\frac{r_{mir}}{d}\Big)^2 + \Big(\frac{405}{216}\cos^2(\phi) - \frac{225}{216}\Big)\Big(\frac{x_{mir}}{d}\Big)^2\Big] \end{aligned} \tag{4}$$

The definition of the parameters are given in Table 1 with their value for the Virgo NCal used during O3.

$G = 6.67430\text{e-}11$ m^3.kg^{-1}.s^{-2}	Gravitational constant
$\rho_{al} = 2805$ kg.m^{-3}	Density of the rotor
$\rho_{mir} = 2202$ kg.m^{-3}	Density of the mirror
$b = 0.0738$ m	Thickness of the rotor
f_{2rot}	Double frequency of the rotor
d	Distance from the center of the rotor to the center of the mirror
$\alpha = \frac{\pi}{2}$	Opening angle of a rotor sector
$r_{max} = 0.095045$ m	Outer radius of the rotor
$r_{min} = 0.032$ m	Inner radius of the rotor
$r_{mir} = 0.175$ m	Radius of the mirror

Table 1: Parameters used in equation 1

2 Numerical model for the NCal-induced mirror motion

Since we would like to estimate the amplitude of the mirror motion to the sub-percent level we need to take into account defaults and real geometry in our model or at least determine their impact on the amplitude of the NCal signal. It is thus convenient to implement a numerical model using a FEA to make more accurate simulations and to estimate the different systematic uncertainties that are at stake. The model and simulations are being developed in C/C++ as a new software called FROMAGE.

2.1 Defining the grid geometry

Our approach consist in splitting the rotor and the mirror into respectively N_{mir} and N_{rot} parts, and then sum the Newtonian forces computed for all the elements of the rotor acting on every element of the mirror. Since the geometry of the mirror and the rotor are based on cylinders we choose to divide both systems into several parts of cylinder defined as shown in Figure 2. Assuming the mirror is split into $n_{mir,x} \times n_{mir,\alpha} \times n_{mir,r}$ elements and one sector[3] of the rotor is split into $n_{rot,y} \times n_{rot,\alpha} \times n_{rot,r}$ elements, the center of mass of a volume element for the mirror

[3]For all that follows, we consider only the sector in the part ($x \geq 0,\ z \geq 0$) but a similar analysis can be done for the second sector which has to be taken into account in the total Newtonian force applied on the mirror. It is also worth mentioning that the method can be applied to n sectors of a rotor.

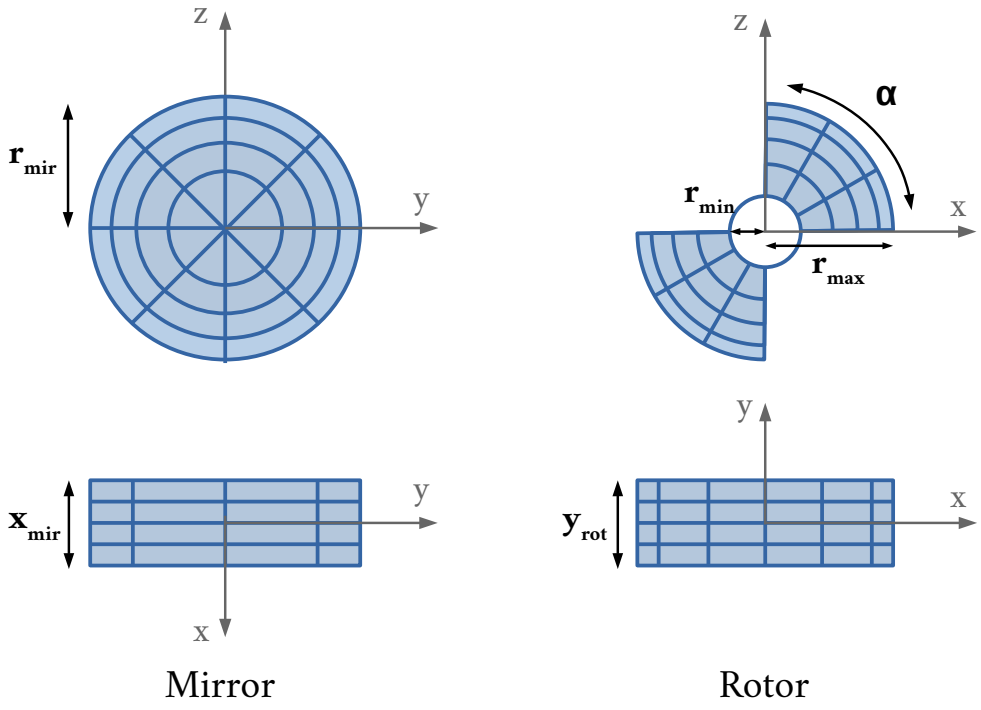

Figure 2: Splitting of the mirror and the NCal rotor using several parts of cylinder.

in the mirror's frame is located at:

$$\begin{pmatrix} x_{mir,i,j,k} \\ y_{mir,i,j,k} \\ z_{mir,i,j,k} \end{pmatrix} = \begin{pmatrix} x_{mir,i,j,k} \\ \frac{2n_{mir,\alpha}}{3\pi}\sin(\frac{\pi}{n_{mir,\alpha}})\frac{R_j^3-R_{j+1}^3}{R_j^2-R_{j+1}^2}\cos(\frac{\pi}{n_{mir,\alpha}}+2k\frac{\pi}{n_{mir,\alpha}}) \\ \frac{2n_{mir,\alpha}}{3\pi}\sin(\frac{\pi}{n_{mir,\alpha}})\frac{R_j^3-R_{j+1}^3}{R_j^2-R_{j+1}^2}\sin(\frac{\pi}{n_{mir,\alpha}}+2k\frac{\pi}{n_{mir,\alpha}}) \end{pmatrix}$$

with:

$$x_{mir,i,j,k} = \begin{cases} \frac{x}{n_{mir,x}}(\frac{1}{2}+i), \text{ if } n_{mir,x} \text{ even and } i < \frac{n_{mir,x}}{2} \\ \frac{x}{n_{mir,x}}i, \text{ if } n_{mir,x} \text{ odd and } i < \frac{n_{mir,x}}{2} \\ -\frac{x}{n_{mir,x}}(\frac{1}{2}+i-\frac{n_{mir,x}}{2}), \text{ if } n_{mir,x} \text{ even and } i \geq \frac{n_{mir,x}}{2} \\ -\frac{x}{n_{mir,x}}(i-\frac{n_{mir,x}}{2}), \text{ if } n_{mir,x} \text{ odd and } i \geq \frac{n_{mir,x}}{2} \end{cases}$$

where $(i,j,k) \in [\![0; n_{mir,x}]\!] \times [\![0; n_{mir,r}]\!] \times [\![0; n_{mir,\alpha}]\!]$ and for the rotor in the rotor's frame:

$$\begin{pmatrix} x'_{rot,i,j,k} \\ y'_{rot,i,j,k} \\ z'_{rot,i,j,k} \end{pmatrix} = \begin{pmatrix} \frac{4n_{rot,\alpha}}{3\alpha}\sin(\frac{\alpha}{2n_{rot,\alpha}})\frac{r_j^3-r_{j+1}^3}{r_j^2-r_{j+1}^2}\cos(\frac{\alpha}{2n_{rot,\alpha}}+k\frac{\alpha}{n_{rot,\alpha}}) \\ \frac{y}{n_{rot,y}}(\frac{1}{2}+i) \text{ if } n_{rot,y} \text{ even}, \frac{y}{n_{rot,y}}i \text{ if } n_{rot,y} \text{ odd} \\ \frac{4n_{rot,\alpha}}{3\alpha}\sin(\frac{\alpha}{2n_{rot,\alpha}})\frac{r_j^3-r_{j+1}^3}{r_j^2-r_{j+1}^2}\sin(\frac{\alpha}{2n_{rot,\alpha}}+k\frac{\alpha}{n_{rot,\alpha}}) \end{pmatrix}$$

with:

$$y'_{rot,i,j,k} = \begin{cases} \frac{y}{n_{rot,y}}(\frac{1}{2}+i), \text{ if } n_{rot,y} \text{ even and } i < \frac{n_{rot,y}}{2} \\ \frac{y}{n_{rot,y}}i, \text{ if } n_{rot,y} \text{ odd and } i < \frac{n_{rot,y}}{2} \\ -\frac{y}{n_{rot,y}}(\frac{1}{2}+i-\frac{n_{rot,y}}{2}), \text{ if } n_{rot,y} \text{ even and } i \geq \frac{n_{rot,y}}{2} \\ -\frac{y}{n_{rot,y}}(i-\frac{n_{rot,y}}{2}), \text{ if } n_{rot,y} \text{ odd and } i \geq \frac{n_{rot,y}}{2} \end{cases}$$

where $(i,j,k) \in [\![0; n_{rot,y}]\!] \times [\![0; n_{rot,r}]\!] \times [\![0; n_{rot,\alpha}]\!]$.
The elements have been chosen to have a constant volume in order to have the same mass. Since the volume dV_{mir} of one element of the mirror is:

$$dV_{mir} = \frac{\pi}{n_{mir,\alpha}} \frac{x}{n_{mir,x}} (R_j^2 - R_{j+1}^2) \tag{5}$$

The relation between the radii is:

$$R_j = R_{mir}\sqrt{1 - \frac{j}{n_{mir,r}}} \tag{6}$$

Similarly for the rotor we have:

$$dV_{rot} = \frac{\alpha}{2n_{rot,\alpha}} \frac{y}{n_{mir,x}} (r_j^2 - r_{j+1}^2) \tag{7}$$

and

$$r_j = \sqrt{\Big(1 - \frac{j}{n_{rot,r}}\Big) r_{max}^2 + \frac{j}{n_{rot,r}} r_{min}^2} \tag{8}$$

2.2 Rotation of the rotor's masses

The mirror's motion is induced by the rotation of the rotor and the amplitude can be extracted if the rotor's masses have turned at least by π around the rotor axis. The angle of rotation θ for both sectors is therefore divided into $n_{rot,\theta}$ steps and the coordinates in the rotor's frame are then changed as:

$$\begin{pmatrix} x'_{rot,i,j,k} \\ y'_{rot,i,j,k} \\ z'_{rot,i,j,k} \end{pmatrix}_\theta = \begin{pmatrix} \frac{4n_{rot,\alpha}}{3\alpha} \sin(\frac{\alpha}{2n_{rot,\alpha}}) \frac{r_j^3 - r_{j+1}^3}{r_j^2 - r_{j+1}^2} \cos(\frac{\alpha}{2n_{rot,\alpha}} + k\frac{\alpha}{n_{rot,\alpha}} + \theta) \\ y'_{rot,i,j,k} \\ \frac{4n_{rot,\alpha}}{3\alpha} \sin(\frac{\alpha}{2n_{rot,\alpha}}) \frac{r_j^3 - r_{j+1}^3}{r_j^2 - r_{j+1}^2} \sin(\frac{\alpha}{2n_{rot,\alpha}} + k\frac{\alpha}{n_{rot,\alpha}} + \theta) \end{pmatrix}$$

2.3 Coordinates in the mirror's frame

In order to compute the Newtonian force from all the elements of the rotor acting on all the elements of the mirror, the coordinates of the rotor have to be converted into the mirror's frame. Since the rotor is in the interferometer plane at a distance d of the mirror and can have

an angle Φ with respect to the interferometer's beam axis, the new coordinates are computed by applying a translation and a rotation as follows:

$$\begin{pmatrix} x_{rot,i,j,k} \\ y_{rot,i,j,k} \\ z_{rot,i,j,k} \end{pmatrix}_\theta = \begin{pmatrix} (x'_{rot,i,j,k} + d)\cos(\Phi) - y'_{rot,i,j,k}\sin(\Phi) \\ (x'_{rot,i,j,k} + d)\sin(\Phi) + y'_{rot,i,j,k}\cos(\Phi) \\ z'_{rot,i,j,k} \end{pmatrix}_\theta$$

Figure 3 shows the rotor of the NCalO3 and an end mirror of Advanced Virgo split into many points located at the center of mass of every element for 8 steps of the angle of rotation θ.

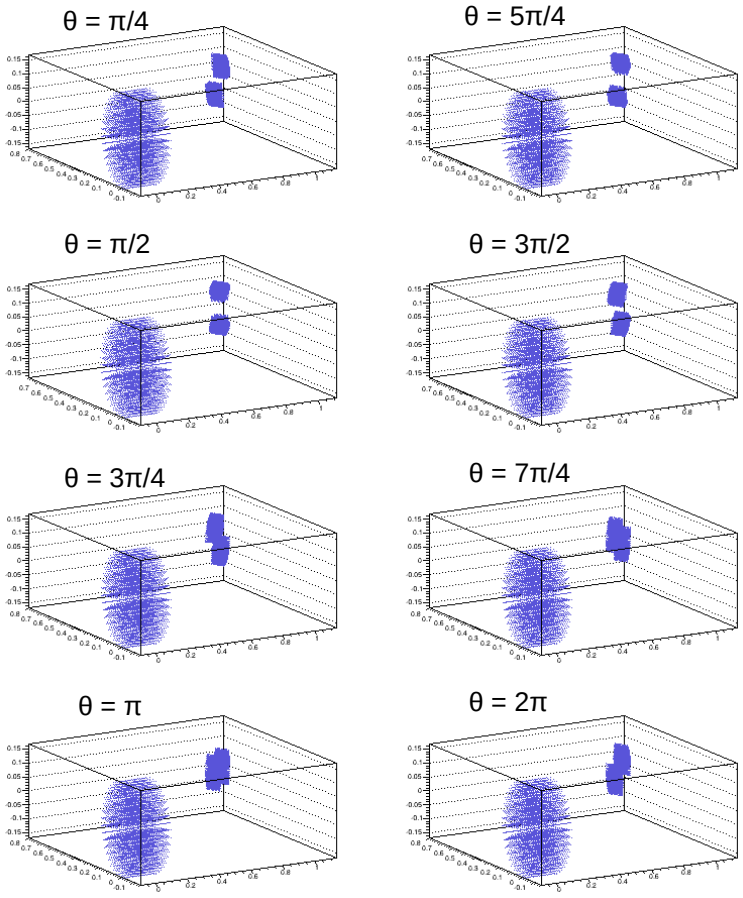

Figure 3: Point cloud of the mirror (foreground) and the rotor (background) when the masses of the rotor are spinning.

2.4 Computation of the Newtonian force

Once all the elements have their coordinates in the common frame it is possible to compute the Newtonian force of the two masses on the mirror for a given angle θ. For clarity reasons, let's

first define $I = (i, j, k)$ for the elements of the mirror and $J = (l, p, q)$ for the elements of one sector of the rotor. The force induced by one sector of the rotor on the mirror is:

$$\vec{F_\theta} = G \sum_I \sum_J \frac{m_{mir,I}\ m_{rot,J}}{d_{I,J}^2} \vec{u}_{I,J} \tag{9}$$

where $m_{mir,I}$ (resp. $m_{rot,J}$) is the mass of the mirror element I (resp. rotor element J), $d_{I,J}$ is the distance between the mirror element I and the rotor element J and $\vec{u}_{I,J}$ is a unit vector along the distance $d_{I,J}$. Since the elements have a constant volume and thus the same mass one gets $m_{mir,I} = m_{mir}$ and $m_{rot,J} = m_{rot}$ and Eq. 9 becomes:

$$\vec{F_\theta} = G m_{mir} m_{rot} \sum_I \sum_J d_{I,J}^{-2} \vec{u}_{I,J} \tag{10}$$

The output signal of the interferometer is primarily sensitive to the longitudinal variations of the end mirrors. Therefore we make a projection of $\vec{F_\theta}$ along the x axis (i.e. the axis of the interferometer's beam):

$$F_{\theta,x} = G m_{mir} m_{rot} \sum_I \sum_J \frac{x_{rot,J} - x_{mir,I}}{d_{I,J}^3} \tag{11}$$

Eventually, the total longitudinal force applied on the mirror is derived by adding also the contributions of the other sectors of the rotor:

$$F_{\theta,x}^{tot} = G m_{mir} m_{rot} \sum_I \sum_J \sum_\mu \frac{x_{rot\mu,J} - x_{mir,I}}{d_{\mu,I,J}^3} \tag{12}$$

where the index $\mu \in [\![1; n_{sectors}]\!]$ with $n_{sectors}$ the number of sectors of the rotor.

2.5 Defining the grid size

The advantage of such a numerical model is that it does not make any approximation on the Newtonian force compared to the analytical model. However, if one wants an infinite precision on the force, the mirror and the rotor should be split into an infinity of elements. As it is not possible in reality, one has to define a grid with enough elements to have a small numerical uncertainty within a reasonable computation time.

We define a grid, called Grid1, of $10 \times 10 \times 10$ elements for the mirror and $10 \times 10 \times 10$ elements for both sectors of the rotor[4]. We then started a converging test for a rotor located at 1.2666 m of the mirror which is the closest location of the NCal to the mirror on Advanced Virgo[5] and

[4]The numbers always refer to what was defined in Sec. 2.1 $n_{mir,x} \times n_{mir,\alpha} \times n_{mir,r}$ and $n_{rot,y} \times n_{rot,\alpha} \times n_{rot,r}$.

[5]This location is where the limitations due to the grid are maximized. Indeed, for increasing distance the grid can be discretized into larger elements since the leading effect on the mirror motion is in d^{-4}.

with an angle $\phi = 0.6058$ with respect to the beam axis[6].

We first started to make an independent sweep for each parameter in the range $[10, 200]$ by 20 log-spaced steps and compute the relative variation of the mirror motion. Figure 4 show the results for all the parameters. It is then possible to define which numerical precision we want to reach on the final result and set the parameters to the associated value. Setting the threshold of relative variation to 0.005% with respect to the asymptotic value per parameter we can build Grid2 from Figure 5 with $12 \times 30 \times 8$ elements for the mirror and $8 \times 65 \times 40$ elements for both sectors of the rotor. We set $n_{mir,r}$ and $n_{rot,y}$ to 8 because the threshold of relative variations at 0.005% of the asymptotic value is already too high for those parameters when starting the converging test from 10. We then repeat the analysis starting with the values of Grid2 and scanning a range $[n_{i,Grid2}, 6n_{i,Grid2}]$ with 10 log-spaced steps. Figure 6 show the results for all the parameters. We can deduce that for simulations purpose and tuning of the model, Grid2 works fine according to Figure 7 since it will give a numerical error $\leq 0.01\%$ which is small enough for the moment (not limiting the NCal uncertainty budget so far) in a reasonable computation time (~ 20 s) when using 8 steps of rotor angle θ in $[0, \frac{7\pi}{8}]$.

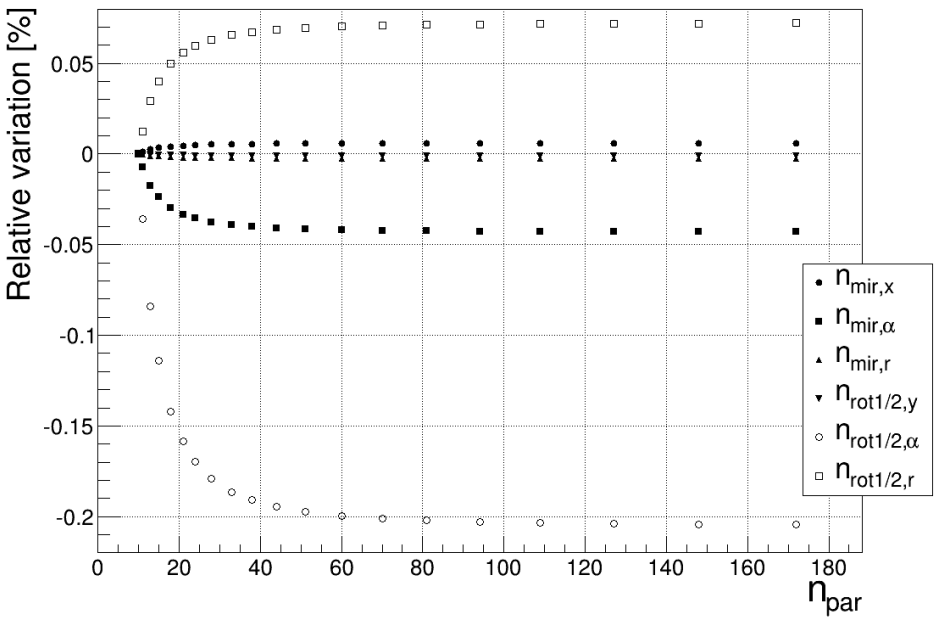

Figure 4: Relative variation of the mirror motion with respect to Grid1 for a logarithmic sweep on the parameters of the mirror and rotor in the range $[10, 200]$. *For the rotor, only one sweep is done for both sectors.*

[6]Real position of the NCal on Advanced Virgo during O3.

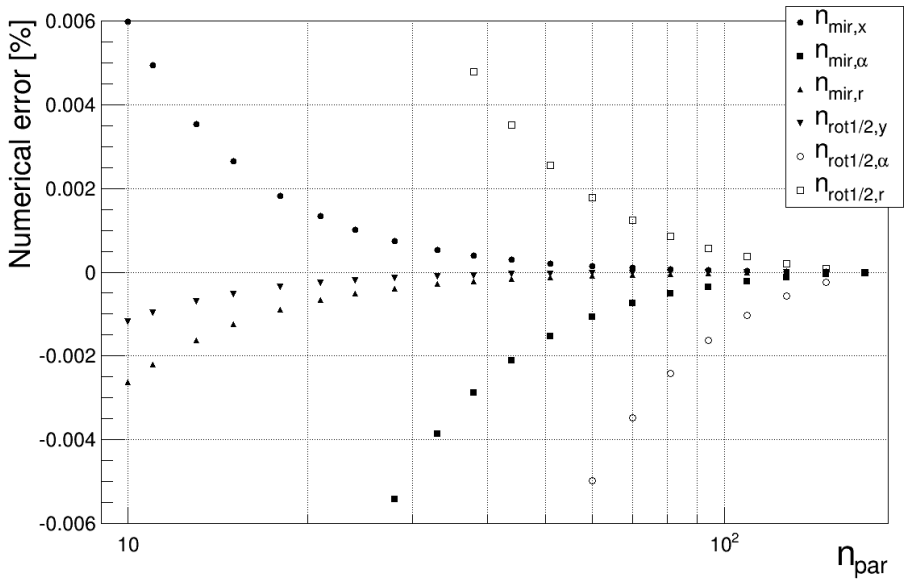

Figure 5: Numerical error on the results for every parameter of the Grid1.

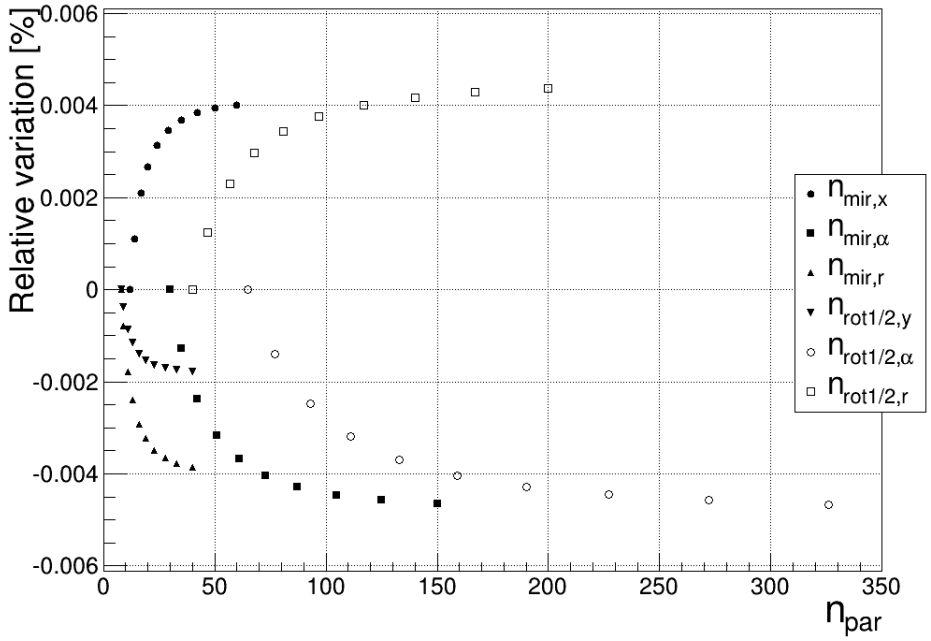

Figure 6: Relative variation of the mirror motion for a sweep on the parameters of the mirror and rotor in the range $[n_{i,Grid2}, 6n_{i,Grid2}]$. For the rotor, only one sweep is done for both sectors.

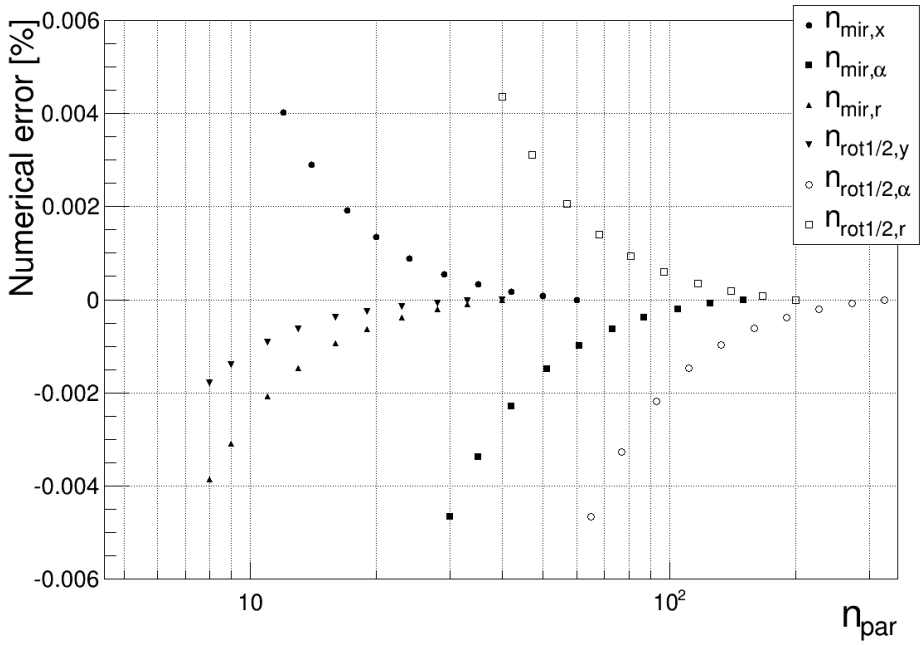

Figure 7: Numerical error on the results for every parameter of the Grid2.

The grid could still be updated, *if needed*, when comparing the simulations to the real data on Advanced Virgo+ and smaller numerical error could be reached with a computation time of a few minutes.

2.6 Amplitude of the mirror motion

The periodic displacement of the mirror X_θ induced by a NCal at a rotor frequency f_{rot} can be expanded in Fourier series such as:

$$X(\theta) = \frac{1}{N}\Big(C_0 + 2\sum_{k=1}^{N-1} |C_k| \cos(k\theta + \psi_k)\Big) \tag{13}$$

with C_k the complex Fourier coefficients, ψ_k the phase of C_k and $\theta = \frac{2\pi f_{rot}}{N}$.
In the case of the Virgo NCalO3 which is made of 2 sectors, only the contribution of the quadrupole moment at twice the rotor frequency (i.e. at 2θ) is expected to be significant in the amplitude of the mirror. In that case the displacement of the mirror X induced by the NCal at twice the rotor frequency f_{2rot} is given by:

$$X(f_{2rot}) = \frac{F^{tot}_{\theta,x}}{M_{mir}(2\pi f_{2rot})^2} \tag{14}$$

where M_{mir} is the mass of the mirror.

Let's define the amplitude of the mirror motion as:

$$a(\theta) = \frac{X_{max} - X_{min}}{2} \tag{15}$$

with X_{max} (resp. X_{min}) the maximum (resp. minimum) value of the mirror's displacement.
In order to verify that the total amplitude of the mirror is mainly the amplitude at twice the rotor frequency and that the other terms are negligible, we compute the Fourier coefficients of the numerical amplitude given by FROMAGE and the residuals at the order 2. Table 2 gives the Fourier coefficients of the numerical mirror strain for the Virgo NCalO3 at a distance 1.2666 m from the mirror, with an angle $\phi = 0.6058$ rad with respect to the interferometer beam axis and at $f_{2rot} = 1$ Hz. C_2 is indeed the main contribution to the total amplitude of the mirror's motion and C_0 is just a time-independent offset. One can also notice that the numerical signal and the signal at f_{2rot} are in phase.

Fourier Coeff.	Amplitude $[h]$	Phase [deg]
C_0	7.52397e-16	0
C_1	2.13463e-30 f_{rot}^{-2}	183
C_2	3.35754e-18 f_{2rot}^{-2}	1e-12
Numerical amplitude	3.35752e-18	–
Residuals	0.0007%	–

Table 2: Fourier coefficients and numerical amplitude of the mirror strain for the Virgo NCalO3 located at a distance $d_N = 1.2666$ m and at the angle $\phi = 0.6058$ rad. The maximum residuals between the numerical amplitude and the sum of the Fourier coefficients is also given.

3 Results

The mirror amplitudes given in this section using the NCalO3 geometry are the amplitudes of the C_2 coefficients as defined in previous section. For each result given, we have checked that the residuals with respect to the total amplitude is negligible.

3.1 Comparison between the analytical and numerical models

We aim at comparing the results we get for the NCal-induced strain on the mirror from the numerical and analytical models. The analytical models will be called "Analytical2" for the formula derived in Eq. 4 and "Analytical1" for the formula used in the analysis presented in VIR-0268A-20. Table 3 show the results computed for the NCal_N (resp. NCal_S) at a distance $d_N = 1.2666$ m (resp. $d_S = 1.9466$ m) of the mirror and for an angle with the interferometer's beam axis of $\phi = 0.6058$ rad (more details on those values are given in VIR-0268A-20).
Several comments can be made on these values:

	(d_N, ϕ)	(d_S, ϕ)
Numerical strain	3.35754e-18 f_{2rot}^{-2}	6.03812e-19 f_{2rot}^{-2}
Analytical1 relative error	-1.09%	-0.46%
Analytical2 relative error	$+0.11\%$	$+0.05\%$

Table 3: Comparison of the computed strain between the numerical and analytical models for the NCal_N and NCal_S located at a distance $d_N = 1.2666$ m and $d_S = 1.9466$ m respectively at the real angle $\phi = 0.6058$ rad. The relative errors given for the analytical models are computed as $(\frac{analytical}{numerical} - 1) \times 100$.

- The numerical and analytical models tend to agree more on their results for larger distance which is indeed expected since the neglected high order terms of the analytical calculation become smaller as d increases.
- Analytical2 model gives closer values to the numerical model than the old Analytical1 model strengthening the fact that the new analytical model is more accurate.
- The geometry used in the numerical model is a simple one and can be tuned further using the rotor drawing and a more realistic geometry of the mirror with the ears and anchors used for its suspension.

3.2 Torque on the mirror

Another feature that may couple to the longitudinal mirror motion sensed by the interferometer's beam is the effect of a NCal-induced torque on the mirror. This can only arise if the beam is not centered on the mirror in which case the angular motion of the mirror couple to the longitudinal mirror motion.
A torque from a force $\vec{F}$ applied on a point P with respect to the center of mass of the mirror O is given by the following equation:

$$\vec{\mathcal{M}}_O(\vec{F}) = \overrightarrow{OP} \times \vec{F} \tag{16}$$

Since we only want to know the torques that affect the longitudinal mirror motion, we need to project the relation onto the y and z axes. As the forces are computed in the mirror's frame, the components $\mathcal{M}_{O,y}$ and $\mathcal{M}_{O,z}$ are directly the torque projections on the y and z axes that we note $\mathcal{M}_y$ and $\mathcal{M}_z$.
Using:

$$\mathcal{M}_i = I_i \cdot \ddot{\theta}_i \tag{17}$$

with $i \in \{x, y, z\}$, I_i the moment of inertia of the mirror along the i axis and $\ddot{\theta}_i$ the angular acceleration around the i axis. Modelling the mirror as a full cylinder the moment of inertia along the y and z axes is the moment of inertia along a central diameter:

$$I_y = I_z = \frac{m_{mir}}{4}\left(r_{mir}^2 + \frac{x_{mir}^2}{3}\right) \tag{18}$$

Then, by integrating Eq. 17 we get:

$$\theta_i = \frac{\mathcal{M}_i}{I_i(2\pi f_{2rot})^2} \tag{19}$$

For small angle θ_i the contribution δ_i of the torque to the displacement of the beam in the longitudinal x axis is given by:

$$\delta_i = \theta_i \cdot b_j \tag{20}$$

where b_j is the beam offset in the direction $j \neq i$.
In Advanced Virgo, the beam is centered on the mirror with an accuracy better than ± 0.5 mm [1]. Considering the worst case scenario where both offsets on y and z are ± 0.5 mm. Table 4 gives the effect of the torque on the mirror longitudinal displacement. The amplitude of the mirror motion is affected by $\pm 0.05\%$. This value will be added to the systematic uncertainty budget of the NCal-induced displacement.
It is interesting to note that for symmetry reasons, a beam offset on the z axis has no effect on the sensed mirror motion when the axis of the rotor is in or orthogonal[7] to the plane of the interferometer.

	(d_N, ϕ)	(d_S, ϕ)
Numerical strain for $b_y = 0$, $b_z = 0$	3.35754e-18 f_{2rot}^{-2}	6.03812e-19 f_{2rot}^{-2}
Variations for $b_y = \pm 0.5$ mm, $b_z = \pm 0.5$ mm	$\mp 0.05\%$	$\mp 0.03\%$

Table 4: Impact of an angular motion of the mirror on the longitudinal displacement of the mirror sensed by a non-centered beam of the interferometer.

3.3 Toward a better modelling of the mirror and the rotor

The Advanced Virgo mirrors are not perfectly cylindrical since there are flat surfaces of 5 cm height in order to fix the ears and hang the mirror with anchors and monolithic suspensions to the marionette as shown in Figure 8. Two ears and four anchors have been modelled with cuboids using the values from [5] and [2] gathered in Table 5.

	Ear	Anchor
Length [mm]	90	39
Thickness [mm]	10	8
Height [mm]	15	8

Table 5: Parameters to define the cuboids to model the ears and anchors.

The rotor is not made of two full sectors but four instead since there is an aluminium plate in between the four empty sectors that only account for an offset in the Newtonian force. Several

[7] Assuming the center of the rotor is in the plane of the interferometer

holes have also been drilled and modelled with cylinders filled with stainless steel screws[8]. Also, the junction between the empty and full sectors are made of mechanical fillets. All the parameters are given in the drawing of the NCalO3 in Figure 9.

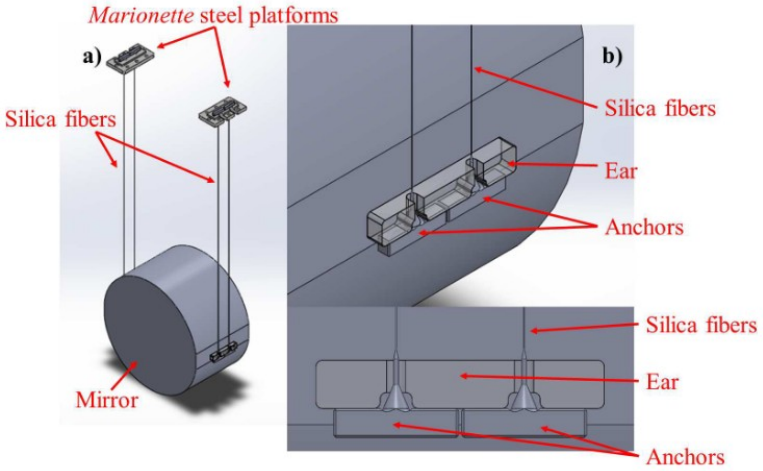

Figure 8: Simulated view of an Advanced Virgo mirror with ears, anchors and monolithic suspensions. Credits: F. Travasso [4]

The aforementioned geometry features for the mirror and the rotor have thus been added to the simulations. Table 6 gives a comparison between the results using the geometry corrections for the mirror and rotor called "Numerical2" model with the previous numerical model called "Numerical1" and both analytical models. The contributions to the amplitude of the mirror displacement for the geometry of the mirror only and for the geometry of the rotor only are also given separately. The fine tuning of both geometries account for less than 0.02% difference with the simpler numerical model.

[8]Density of stainless steel is 8000 kg/m^3

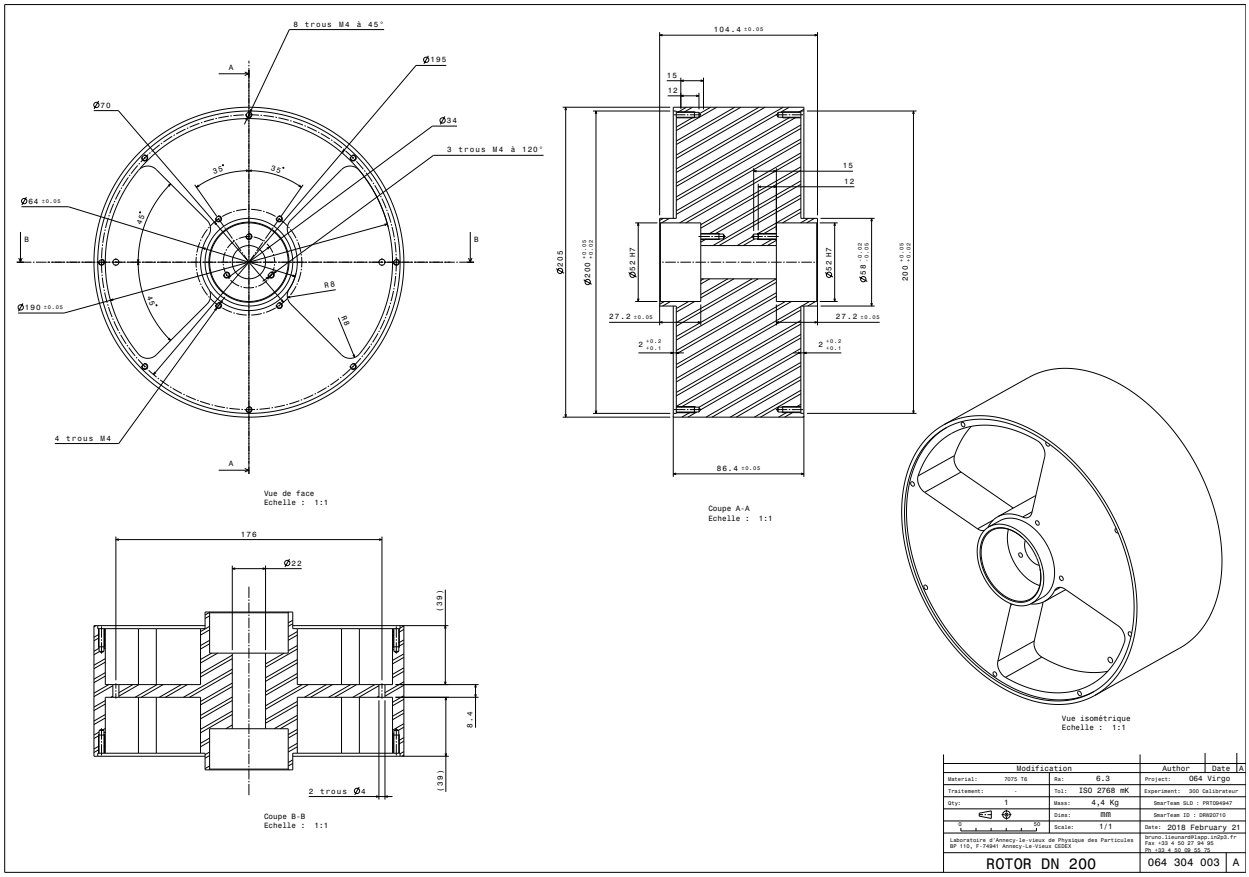

Figure 9: Drawing of the NCalO3 rotor.

	(d_N, ϕ)	(d_S, ϕ)
Numerical2 strain	3.35721e-18 f_{2rot}^{-2}	6.03901e-19 f_{2rot}^{-2}
Numerical1 strain	$+0.01\%$	-0.015%
Analytical1 relative error	-1.08%	-0.47%
Analytical2 relative error	$+0.12\%$	$+0.03\%$
Numerical2M strain	3.3577e-18 f_{2rot}^{-2}	6.03824e-19 f_{2rot}^{-2}
Numerical2R strain	3.35706e-18 f_{2rot}^{-2}	6.03889e-19 f_{2rot}^{-2}

Table 6: Comparison of the computed strain between the numerical and analytical models for the NCal_N and NCal_S located at a distance $d_N = 1.2666$ m and $d_S = 1.9466$ m respectively at the real angle $\phi = 0.6058$ rad. The relative errors given for the analytical models are computed as $(\frac{Model}{Numerical2} - 1) \times 100$. The amplitude for the single correction of the mirror geometry (Numerical2M) and the rotor geometry (Numerical2R) are also given.

3.4 Reaching higher frequency

The current NCal with two sectors on Virgo can spin up to $\sim$ 100 Hz which gives a signal at 200 Hz at maximum. If we want to verify the reconstruction of $h(t)$ at higher frequency a simple idea is to increase the angular speed of the rotor or increase the number of sectors of the NCal. If $n_{sectors} = 3$, a hexapole moment is generated and the mirror's motion is at three times the rotor frequency. This means that with the current masses of the Virgo NCal and the speed limits on the rotor spin, a three fold NCal could give a signal up to 300 Hz.
We have thus computed with FROMAGE the amplitude of the mirror motion using a three fold NCal and we got a numerical strain for the NCal_N position of $h_N = 2.24399\text{e-}19 f_{3rot}^{-2}$ with $f_{3rot} = 3f_{rot}$. Comparing this result to the result with the current NCal $h_N = 3.35754\text{e-}18 f_{2rot}^{-2}$, the amplitude is suppressed by a factor ~ 15.
In conclusion, a gain of 50% on the frequency requires to spin masses 15 times heavier than the current ones to reach similar amplitudes in the same amount of time. Investigations on whether it is more reasonable to spin a 2 fold NCal 50% faster or to spin a 3 fold NCal 15 times heavier at the current speed are on-going.

3.5 LIGO NCal prototype

LIGO is also developing its own NCal prototype -v1 at Hanford. Using their parameters we have been able to extract the different values of the force expected on their end test mass at the quadrupole, hexapole, octopole and dodecapole moments. The values are gathered in Table 7. Private exchange with M.P. Ross indicates an agreement with their numerical values (using FEA) better than 0.07%.

Moments	Force [N_{pk}]	Strain
2f	1.96333e-11	3.13505e-18 f_{2rot}^{-2}
3f	9.3326e-12	1.49023e-18 f_{3rot}^{-2}
4f	4.9853e-14	7.96051e-21 f_{4rot}^{-2}
6f	6.80053e-15	1.08591e-21 f_{6rot}^{-2}

Table 7: Force and strain induced by the LIGO NCal prototype -v1 on an end test mass at LHO.

4 Extracting the absolute distance with two NCals

The main contribution to the systematic uncertainty budget of the NCal is the absolute distance between the mirror and the rotor (see VIR-0268A-20). It is possible to extract the offset between the real distance and the distance used to compute the amplitude of the mirror motion using two NCals separated by a fixed known distance. On Advanced Virgo, two NCalO3 were installed on a rigid support separated by 54 cm. Their estimated distance to the mirror were $d_N = 1.2666$ m

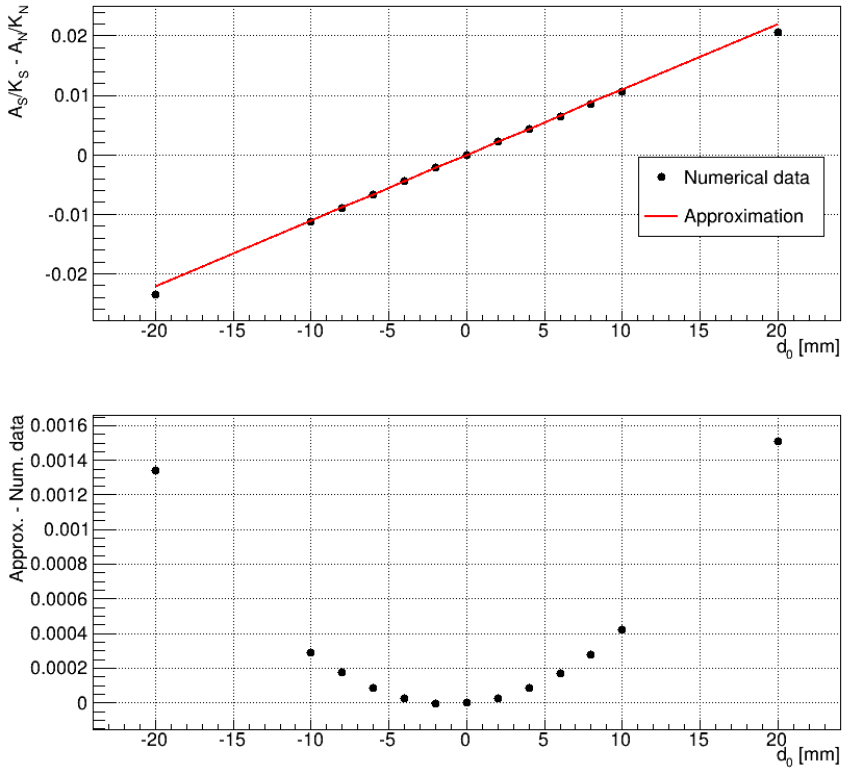

Figure 10: Comparison between the linear approximation of Eq .23 and the numerical results computed with FROMAGE.

and $d_S = 1.9466$ m. Assuming that the real distances differ from the estimated distances by an offset d_0, it is possible to predict the difference between both NCal signal amplitudes as a function of d_0. We give below an analytical approximation of this function.
Let's call A_i the amplitude of the mirror motion induced by the NCal_i with $i = \{N, S\}$. The real amplitude at the second order of the gravitational force can be expressed as:

$$A_i = C_i(d_i + d_0)^{-4} \tag{21}$$

with C_i the gravitational coupling factor. From Eq. 21 and assuming $d_0 \ll d_i$ we can write:

$$A_i \approx K_i(1 - 4\frac{d_0}{d_i}) \tag{22}$$

with K_i the amplitude of the mirror motion computed with a rotor at the estimated distance d_i from the mirror. The difference of the ratios between the real amplitude A and the estimated amplitude K of both NCals is:

$$\frac{A_S}{K_S} - \frac{A_N}{K_N} = 4d_0\frac{d_S - d_N}{d_S \cdot d_N} \approx 1.103\ d_0 \tag{23}$$

One can check that this approximation holds for small offsets d_0, typically smaller than 1 cm, using FROMAGE. Figure 10 shows the comparison between the numerical results and the approximation of Eq. 23. The linear approximation is in agreement with the numerical results within better than 0.05% for any offset $d_0 \leq 1$ cm.

Conclusion

The new software FROMAGE has been developed to make simulations using FEA. The v1r0 version of the software offers the possibility to model many NCal geometries and can be applied on both Virgo and LIGO NCals.

The numerical grid has been defined for the Virgo NCalO3 such that the results do not differ from a quasi-infinite precision result by less than 0.01%. The main parameters that impact the results are the angular and radial discretization of the rotor ($n_{rot1/2,\alpha}$ and $n_{rot1/2,r}$) and the angular discretization of the mirror ($n_{mir,\alpha}$). The grid could have a better resolution to give more precise results within a reasonable computation time (a few minutes) if it is needed in the future.

In order to be confident that the amplitude of the signal induced by the rotor is at the expected frequency, we extract the amplitude of the Fourier series of the numerical signal and compute the residuals.

The NCal-induced torque on the mirror affects the amplitude of the mirror motion at the level of 0.05% for a beam offset of 0.5 mm. Note that the dependence on the beam offset is linear.

Eventually we have also shown that tuning the geometry of the mirror and the rotor in a more realistic way does not impact significantly the results ($\leq 0.02\%$) compared to simpler geometry approximations.

Now the pending question that remains is "how far our model is from reality?". In order to assess this, we use the latest analytical results that we have at our disposal and compare them to the numerical results. The differences between both models are 0.12% and 0.03% for the NCal_N and NCal_S respectively. Future discussions with LIGO folks and comparison with their models could also be helpful to estimate this uncertainty.

We give in Table 8 the list of systematic uncertainties of the numerical model computed with FROMAGE[9] on the NCal-induced mirror motion. The total relative uncertainty of the numerical model has been estimated to 0.13% and 0.05% for the NCal_N and NCal_S respectively.

[9]The results have been obtained with the version v1r0 of FROMAGE.

One can notice that the errors induced by geometrical approximations for the NCalO3 numerical results are smaller, as expected, than the difference between the analytical model (simple geometry) and the numerical model (realistic geometry).

Parameter	Relative impact [%] (d_N, ϕ)	Relative impact [%] (d_S, ϕ)
Numerical grid	≤ 0.01	≤ 0.01
Torque (± 0.5 mm)	0.05	0.03
Geometry approx. NCalO3	0.01	≤ 0.02
Analytical2/Numerical2	0.12	0.03
Total (quadratic sum)	~ 0.13	~ 0.05

Table 8: Estimation of uncertainties on the NCal-induced mirror motion due to the numerical model computed with FROMAGE both for the NCal_N and NCal_S.

References

[1] J. Casanueva Diaz. Control of the gravitational wave interferometric detector Advanced Virgo. *Thesis*, 2017.

[2] E. Hennes and P. Puppo. Fem stress study of the anchors of the monolithic suspensions in the setup used for the breaking test. *VIR-0375B-16*, 2016.

[3] B. Mours and T. Pradier. Analysis of the NCal data collected during O3B. *VIR-0268A-20*, 2020.

[4] F Travasso and Virgo Collaboration. Status of the Monolithic Suspensions for Advanced Virgo. *Journal of Physics: Conference Series*, 957:012012, 02 2018.

[5] F. Travasso and H. Vocca. Technical designs of ears and anchors. *VIR-0228A-16*, 2016.